Physics Letters B 318 (1993) 249–262
North-Holland

PHYSICS LETTERS B

Production of Λ and $\Lambda\overline{\Lambda}$ correlations in the hadronic decays of the Z^0

DELPHI Collaboration

P. Abreu [t], W. Adam [g], T. Adye [ak], E. Agasi [ad], R. Aleksan [am], G.D. Alekseev [n], A. Algeri [m], P. Allen [aw], S. Almehed [w], S.J. Alvsvaag [d], U. Amaldi [g], A. Andreazza [aa], P. Antilogus [x], W-D. Apel [o], R.J. Apsimon [ak], Y. Arnoud [am], B. Åsman [as], J-E. Augustin [r], A. Augustinus [ad], P. Baillon [g], P. Bambade [r], F. Barao [t], R. Barate [ℓ], G. Barbiellini [au], D.Y. Bardin [n], G.J. Barker [ah], A. Baroncelli [ao], O. Barring [g], J.A. Barrio [y], W. Bartl [ay], M.J. Bates [ak], M. Battaglia [m], M. Baubillier [v], K-H. Becks [ba], M. Begalli [aj], P. Beilliere [f], Yu. Belokopytov [aq], P. Beltran [i], D. Benedic [h], A.C. Benvenuti [e], M. Berggren [r], D. Bertrand [b], F. Bianchi [at], M.S. Bilenky [n], P. Billoir [v], J. Bjarne [w], D. Bloch [h], J. Blocki [az], S. Blyth [ah], V. Bocci [aℓ], P.N. Bogolubov [n], T. Bolognese [am], M. Bonesini [aa], W. Bonivento [aa], P.S.L. Booth [u], G. Borisov [aq], H. Borner [g], C. Bosio [ao], B. Bostjancic [ar], S. Bosworth [ah], O. Botner [av], E. Boudinov [aq], B. Bouquet [r], C. Bourdarios [r], T.J.V. Bowcock [u], M. Bozzo [k], S. Braibant [b], P. Branchini [ao], K.D. Brand [ai], R.A. Brenner [g], H. Briand [v], C. Bricman [b], L. Brillault [v], R.C.A. Brown [g], P. Bruckman [p], J-M. Brunet [f], A. Budziak [p], L. Bugge [af], T. Buran [af], H. Burmeister [g], J.A.M.A. Buytaert [g], M. Caccia [g], M. Calvi [aa], A.J. Camacho Rozas [ap], R. Campion [u], T. Camporesi [g], V. Canale [aℓ], F. Cao [b], F. Carena [g], L. Carroll [u], M.V. Castillo Gimenez [aw], A. Cattai [g], F.R. Cavallo [e], L. Cerrito [aℓ], V. Chabaud [g], A. Chan [a], Ph. Charpentier [g], L. Chaussard [r], J. Chauveau [v], P. Checchia [ai], G.A. Chelkov [n], L. Chevalier [am], P. Chliapnikov [aq], V. Chorowicz [v], J.T.M. Chrin [aw], V. Cindro [ar], P. Collins [ah], J.L. Contreras [y], R. Contri [k], E. Cortina [aw], G. Cosme [r], F. Couchot [r], H.B. Crawley [a], D. Crennell [ak], G. Crosetti [k], J. Cuevas Maestro [ag], S. Czellar [m], E. Dahl-Jensen [ab], B. Dalmagne [r], M. Dam [af], G. Damgaard [ab], G. Darbo [k], E. Daubie [b], A. Daum [o], P.D. Dauncey [ah], M. Davenport [g], J. Davies [u], W. Da Silva [v], C. Defoix [f], P. Delpierre [z], N. Demaria [at], A. De Angelis [au], H. De Boeck [b], W. De Boer [o], S. De Brabandere [b], C. De Clercq [b], M.D.M. De Fez Laso [aw], C. De La Vaissiere [v], B. De Lotto [au], A. De Min [aa], H. Dijkstra [g], L. Di Ciaccio [aℓ], J. Dolbeau [f], M. Donszelmann [g], K. Doroba [az], M. Dracos [g], J. Drees [ba], M. Dris [ae], Y. Dufour [g], F. Dupont [ℓ], D. Edsall [a], L-O. Eek [av], P.A.-M. Eerola [g], R. Ehret [o], T. Ekelof [av], G. Ekspong [as], A. Elliot Peisert [ai], M. Elsing [ba], J-P. Engel [h], N. Ershaidat [v], M. Espirito Santo [t], V. Falaleev [aq], D. Fassouliotis [ae], M. Feindt [g], A. Ferrer [aw], T.A. Filippas [ae], A. Firestone [a], H. Foeth [g], E. Fokitis [ae], F. Fontanelli [k], K.A.J. Forbes [u], J-L. Fousset [z], S. Francon [x], B. Franek [ak], P. Frenkiel [f], D.C. Fries [o], A.G. Frodesen [d], F. Fulda-Quenzer [r], H. Furstenau [o], J. Fuster [g], D. Gamba [at], C. Garcia [aw], J. Garcia [ap], C. Gaspar [g], U. Gasparini [ai], Ph. Gavillet [g], E.N. Gazis [ae], J-P. Gerber [h], P. Giacomelli [g], D. Gillespie [g], R. Gokieli [az], B. Golob [ar], V.M. Golovatyuk [n], J.J. Gomez Y Cadenas [g], G. Gopal [ak], L. Gorn [a], M. Gorski [az], V. Gracco [k], A. Grant [g], F. Grard [b], E. Graziani [ao], G. Grosdidier [r], E. Gross [g], B. Grossetete [v], S. Gumenyuk [aq], J. Guy [ak], U. Haedinger [o], F. Hahn [ba], M. Hahn [o], S. Haider [ad], Z. Hajduk [p], A. Hakansson [w], A. Hallgren [av], K. Hamacher [ba], G. Hamel De Monchenault [am], W. Hao [ad], F.J. Harris [ah], V. Hedberg [w], T. Henkes [g], R. Henriques [t], J.J. Hernandez [aw], P. Herquet [b], H. Herr [g], T.L. Hessing [u], I. Hietanen [m], C.O. Higgins [u], E. Higon [aw], H.J. Hilke [g], S.D. Hodgson [ah], T. Hofmokl [az], S-O. Holmgren [as], P.J. Holt [ah], D. Holthuizen [ad], P.F. Honore [f], M. Houlden [u], J. Hrubec [ay], K. Huet [b], P.O. Hulth [as], K. Hultqvist [as], P. Ioannou [c], P-S. Iversen [d], J.N. Jackson [u],

P. Jalocha [p], G. Jarlskog [w], P. Jarry [am], B. Jean-Marie [r], E.K. Johansson [as], M. Jonker [g], L. Jonsson [w], P. Juillot [h], G. Kalkanis [c], G. Kalmus [ak], F. Kapusta [v], M. Karlsson [g], E. Karvelas [i], S. Katsanevas [c], E.C. Katsoufis [ae], R. Keranen [g], B.A. Khomenko [n], N.N. Khovanski [n], B. King [u], N.J. Kjaer [g], H. Klein [g], A. Klovning [d], P. Kluit [ad], A. Koch-Mehrin [ba], J.H. Koehne [o], B. Koene [ad], P. Kokkinias [i], M. Koratzinos [af], K. Korcyl [p], A.V. Korytov [n], V. Kostioukhine [aq], C. Kourkoumelis [c], O. Kouznetsov [n], P.H. Kramer [ba], M. Krammer [ay], C. Kreuter [o], J. Krolikowski [az], I. Kronkvist [w], U. Kruener-Marquis [ba], W. Kucewicz [p], K. Kulka [av], K. Kurvinen [m], C. Lacasta [aw], C. Lambropoulos [i], J.W. Lamsa [a], L. Lanceri [au], V. Lapin [aq], I. Last [u], J-P. Laugier [am], R. Lauhakangas [m], G. Leder [ay], F. Ledroit [ℓ], R. Leitner [ac], Y. Lemoigne [am], J. Lemonne [b], G. Lenzen [ba], V. Lepeltier [r], T. Lesiak [p], J.M. Levy [h], E. Lieb [ba], D. Liko [ay], J. Lindgren [m], R. Lindner [ba], I. Lippi [ai], B. Loerstad [w], M. Lokajicek [j], J.G. Loken [ah], A. Lopez-Fernandez [g], M.A. Lopez Aguera [ap], M. Los [ad], D. Loukas [i], J.J. Lozano [aw], P. Lutz [f], L. Lyons [ah], G. Maehlum [af], J. Maillard [f], A. Maio [t], A. Maltezos [i], F. Mandl [ay], J. Marco [ap], M. Margoni [ai], J-C. Marin [g], A. Markou [i], T. Maron [ba], S. Marti [aw], C. Martinez-Rivero [ap], F. Matorras [ap], C. Matteuzzi [aa], G. Matthiae [aℓ], M. Mazzucato [ai], M. Mc Cubbin [u], R. Mc Kay [a], R. Mc Nulty [u], J. Medbo [av], G. Meola [k], C. Meroni [aa], W.T. Meyer [a], M. Michelotto [ai], I. Mikulec [ay], L. Mirabito [x], W.A. Mitaroff [ay], G.V. Mitselmakher [n], U. Mjoernmark [w], T. Moa [as], R. Moeller [ab], K. Moenig [g], M.R. Monge [k], P. Morettini [k], H. Mueller [o], W.J. Murray [ak], G. Myatt [ah], F.L. Navarria [e], P. Negri [aa], S. Nemecek [j], R. Nicolaidou [c], B.S. Nielsen [ab], B. Nijjhar [u], V. Nikolaenko [aq], P.E.S. Nilsen [d], P. Niss [as], A. Nomerotski [ai], V. Obraztsov [aq], A.G. Olshevski [n], R. Orava [m], A. Ostankov [aq], K. Osterberg [m], A. Ouraou [am], M. Paganoni [aa], R. Pain [v], H. Palka [p], Th.D. Papadopoulou [ae], L. Pape [g], F. Parodi [k], A. Passeri [ao], M. Pegoraro [ai], J. Pennanen [m], L. Peralta [t], H. Pernegger [ay], M. Pernicka [ay], A. Perrotta [e], C. Petridou [au], A. Petrolini [k], G. Piana [k], F. Pierre [am], M. Pimenta [t], S. Plaszczynski [r], O. Podobrin [o], M.E. Pol [q], G. Polok [p], P. Poropat [au], V. Pozdniakov [n], P. Privitera [aℓ], A. Pullia [aa], D. Radojicic [ah], S. Ragazzi [aa], H. Rahmani [ae], J. Rames [j], P.N. Ratoff [s], A.L. Read [af], P. Rebecchi [g], N.G. Redaelli [aa], M. Regler [ay], D. Reid [g], P.B. Renton [ah], L.K. Resvanis [c], F. Richard [r], J. Richardson [u], J. Ridky [j], G. Rinaudo [at], I. Roditi [q], A. Romero [at], I. Roncagliolo [k], P. Ronchese [ai], C. Ronnqvist [m], E.I. Rosenberg [a], E. Rosso [g], P. Roudeau [r], T. Rovelli [e], W. Ruckstuhl [ad], V. Ruhlmann-Kleider [am], A. Ruiz [ap], H. Saarikko [m], Y. Sacquin [am], G. Sajot [ℓ], J. Salt [aw], J. Sanchez [y], M. Sannino [k,an], S. Schael [g], H. Schneider [o], M.A.E. Schyns [ba], G. Sciolla [at], F. Scuri [au], A.M. Segar [ah], A. Seitz [o], R. Sekulin [ak], M. Sessa [au], R. Seufert [o], R.C. Shellard [aj], I. Siccama [ad], P. Siegrist [am], S. Simonetti [k], F. Simonetto [ai], A.N. Sisakian [n], G. Skjevling [af], G. Smadja [am,x], O. Smirnova [n], G.R. Smith [ak], R. Sosnowski [az], D. Souza-Santos [aj], T. Spassov [t], E. Spiriti [ao], S. Squarcia [k], H. Staeck [ba], C. Stanescu [ao], S. Stapnes [af], G. Stavropoulos [i], F. Stichelbaut [b], A. Stocchi [r], J. Strauss [ay], J. Straver [g], R. Strub [h], B. Stugu [d], M. Szczekowski [g], M. Szeptycka [az], P. Szymanski [az], T. Tabarelli [aa], O. Tchikilev [aq], G.E. Theodosiou [i], A. Tilquin [z], J. Timmermans [ad], V.G. Timofeev [n], L.G. Tkatchev [n], T. Todorov [h], D.Z. Toet [ad], O. Toker [m], A. Tomaradze [b], B. Tome [t], E. Torassa [at], L. Tortora [ao], D. Treille [g], W. Trischuk [g], G. Tristram [f], C. Troncon [aa], A. Tsirou [g], E.N. Tsyganov [n], M-L. Turluer [am], T. Tuuva [m], I.A. Tyapkin [v], M. Tyndel [ak], S. Tzamarias [u], S. Ueberschaer [ba], O. Ullaland [g], V. Uvarov [aq], G. Valenti [e], E. Vallazza [at], J.A. Valls Ferrer [aw], C. Vander Velde [b], G.W. Van Apeldoorn [ad], P. Van Dam [ad], M. Van Der Heijden [ad], W.K. Van Doninck [b], J. Van Eldik [ad], P. Vaz [g], G. Vegni [aa], L. Ventura [ai], W. Venus [ak], F. Verbeure [b], M. Verlato [ai], L.S. Vertogradov [n], D. Vilanova [am], P. Vincent [x], L. Vitale [m], E. Vlasov [aq], A.S. Vodopyanov [n], M. Vollmer [ba], M. Voutilainen [m], V. Vrba [ao], H. Wahlen [ba], C. Walck [as], F. Waldner [au], A. Wehr [ba], M. Weierstall [ba], P. Weilhammer [g], A.M. Wetherell [g], J.H. Wickens [b], G.R. Wilkinson [ah], W.S.C. Williams [ah],

M. Winter[h], M. Witek[p], G. Wormser[r], K. Woschnagg[av], N. Yamdagni[as], P. Yepes[g], A. Zaitsev[aq], A. Zalewska[p], P. Zalewski[r], M. Zanin[au], D. Zavrtanik[ar], E. Zevgolatakos[i], N.I. Zimin[n], M. Zito[am], D. Zontar[ar], R. Zuberi[ah], G. Zumerle[ai] and J. Zuniga[aw]

[a] *Ames Laboratory and Department of Physics, Iowa State University, Ames IA 50011, USA*
[b] *Physics Department, Univ. Instelling Antwerpen, Universiteitsplein 1, B-2610 Wilrijk, Belgium and IIHE, ULB-VUB, Pleinlaan 2, B-1050 Brussels, Belgium and Faculté des Sciences, Univ. de l'Etat Mons, Av. Maistriau 19, B-7000 Mons, Belgium*
[c] *Physics Laboratory, University of Athens, Solonos Str. 104, GR-10680 Athens, Greece*
[d] *Department of Physics, University of Bergen, Allégaten 55, N-5007 Bergen, Norway*
[e] *Dipartimento di Fisica, Università di Bologna and INFN, Via Irnerio 46, I-40126 Bologna, Italy*
[f] *Collège de France, Lab. de Physique Corpusculaire, IN2P3-CNRS, F-75231 Paris Cedex 05, France*
[g] *CERN, CH-1211 Geneva 23, Switzerland*
[h] *Centre de Recherche Nucléaire, IN2P3 - CNRS/ULP - BP20, F-67037 Strasbourg Cedex, France*
[i] *Institute of Nuclear Physics, N.C.S.R. Demokritos, P.O. Box 60228, GR-15310 Athens, Greece*
[j] *FZU, Inst. of Physics of the C.A.S. High Energy Physics Division, Na Slovance 2, CS-180 40, Praha 8, Czechoslovakia*
[k] *Dipartimento di Fisica, Università di Genova and INFN, Via Dodecaneso 33, I-16146 Genova, Italy*
[ℓ] *Institut des Sciences Nucléaires, IN2P3-CNRS, Université de Grenoble 1, F-38026 Grenoble, France*
[m] *Research Institute for High Energy Physics, SEFT, Siltavuorenpenger 20C, SF-00170 Helsinki, Finland*
[n] *Joint Institute for Nuclear Research, Dubna, Head Post Office, P.O. Box 79, 101 000 Moscow, Russian Federation*
[o] *Institut für Experimentelle Kernphysik, Universität Karlsruhe, Postfach 6980, D-7500 Karlsruhe 1, Germany*
[p] *High Energy Physics Laboratory, Institute of Nuclear Physics, Ul. Kawiory 26a, PL-30055 Krakow 30, Poland*
[q] *Centro Brasileiro de Pesquisas Físicas, rua Xavier Sigaud 150, RJ-22290 Rio de Janeiro, Brazil*
[r] *Université de Paris-Sud, Lab. de l'Accélérateur Linéaire, IN2P3-CNRS, Bat 200, F-91405 Orsay, France*
[s] *School of Physics and Materials, University of Lancaster, Lancaster LA1 4YB, UK*
[t] *LIP, IST, FCUL - Av. Elias Garcia, 14 1-o, P-1000 Lisboa Codex, Portugal*
[u] *Department of Physics, University of Liverpool, P.O. Box 147, Liverpool L69 3BX, UK*
[v] *LPNHE, IN2P3-CNRS, Universités Paris VI et VII, Tour 33 (RdC), 4 place Jussieu, F-75252 Paris Cedex 05, France*
[w] *Department of Physics, University of Lund, Sölvegatan 14, S-22363 Lund, Sweden*
[x] *Université Claude Bernard de Lyon, IPNL, IN2P3-CNRS, F-69622 Villeurbanne Cedex, France*
[y] *Universidad Complutense, Avda. Complutense s/n, E-28040 Madrid, Spain*
[z] *Univ. d'Aix - Marseille II - CPP, IN2P3-CNRS, F-13288 Marseille Cedex 09, France*
[aa] *Dipartimento di Fisica, Università di Milano and INFN, Via Celoria 16, I-20133 Milan, Italy*
[ab] *Niels Bohr Institute, Blegdamsvej 17, DK-2100 Copenhagen Ø, Denmark*
[ac] *NC, Nuclear Centre of MFF, Charles University, Areal MFF, V Holesovickach 2, CS-180 00, Praha 8, Czechoslovakia*
[ad] *NIKHEF-H, Postbus 41882, NL-1009 DB Amsterdam, The Netherlands*
[ae] *National Technical University, Physics Department, Zografou Campus, GR-15773 Athens, Greece*
[af] *Physics Department, University of Oslo, Blindern, N-1000 Oslo 3, Norway*
[ag] *Dpto. Fisica, Univ. Oviedo, C/P Jimenez Casas, S/N-33006 Oviedo, Spain*
[ah] *Department of Physics, University of Oxford, Keble Road, Oxford OX1 3RH, UK*
[ai] *Dipartimento di Fisica, Università di Padova and INFN, Via Marzolo 8, I-35131 Padua, Italy*
[aj] *Depto. de Fisica, Pontificia Univ. Católica, C.P. 38071 RJ-22453 Rio de Janeiro, Brazil*
[ak] *Rutherford Appleton Laboratory, Chilton, Didcot OX11 OQX, UK*
[aℓ] *Dipartimento di Fisica, Università di Roma II and INFN, Tor Vergata, I-00173 Rome, Italy*
[am] *Centre d'Etude de Saclay, DSM/DAPNIA, F-91191 Gif-sur-Yvette Cedex, France*
[an] *Dipartimento di Fisica-Università di Salerno, I-84100 Salerno, Italy*
[ao] *Istituto Superiore di Sanità, Ist. Naz. di Fisica Nucl. (INFN), Viale Regina Elena 299, I-00161 Rome, Italy*
[ap] *C.E.A.F.M., C.S.I.C. - Univ. Cantabria, Avda. los Castros, S/N-39006 Santander, Spain*
[aq] *Inst. for High Energy Physics, Serpukov P.O. Box 35, Protvino (Moscow Region), Russian Federation*
[ar] *J. Stefan Institute and Department of Physics, University of Ljubljana, Jamova 39, SI-61000 Ljubljana, Slovenia*
[as] *Fysikum, Stockholm University, Box 6730, S-113 85 Stockholm, Sweden*
[at] *Dipartimento di Fisica Sperimentale, Università di Torino and INFN, Via P. Giuria 1, I-10125 Turin, Italy*
[au] *Dipartimento di Fisica, Università di Trieste and INFN, Via A. Valerio 2, I-34127 Trieste, Italy and Istituto di Fisica, Università di Udine, I-33100 Udine, Italy*
[av] *Department of Radiation Sciences, University of Uppsala, P.O. Box 535, S-751 21 Uppsala, Sweden*
[aw] *IFIC, Valencia-CSIC, and D.F.A.M.N., U. de Valencia, Avda. Dr. Moliner 50, E-46100 Burjassot (Valencia), Spain*

[ay] *Institut für Hochenergiephysik, Österr. Akad. d. Wissensch., Nikolsdorfergasse 18, A-1050 Vienna, Austria*
[az] *Inst. Nuclear Studies and University of Warsaw, Ul. Hoza 69, PL-00681 Warsaw, Poland*
[ba] *Fachbereich Physik, University of Wuppertal, Postfach 100 127, D-5600 Wuppertal 1, Germany*

Received 28 September 1993
Editor: K. Winter

An analysis of the production of the Λ baryon in the hadronic decays of the Z^0 is presented, based on about 993K multihadronic events collected by the DELPHI detector at LEP during 1991 and 1992. The differential cross section of the Λ and the correlations between Λ and $\overline{\Lambda}$ produced in the same event are compared to current models, based both on string fragmentation and on cluster decay. The predictions of the string fragmentation model are found to give satisfactory agreements with the data, clearly better than those of the cluster model.

1. Introduction

The direct production of baryons in e^+e^- annihilations at the Z^0 may be described by many different mechanisms. Among them are the following:

(i) Baryons can come from the recombination of triplets of quarks (q) separately created (fig. 1a). Baryons and antibaryons in the final state should be uncorrelated.

(ii) The Z^0 decay gives rise to a diquark–antidiquark ($D\overline{D}$) pair. The baryon and the antibaryon should be leading particles in opposite jets (fig. 1b).

(iii) Baryons can be produced from diquark–antidiquark pairs in the fragmentation. In this case the baryon–antibaryon pair is expected to be close in phase space, and in general in the same jet. However the production of diquarks should be suppressed with respect to the production of quarks, because of their higher mass (fig. 1c).

(iv) Baryons can be produced from diquarks in the fragmentation, with the possibility that a gap in the string, due to the creation of a $D\overline{D}$ pair, is broken by a $q\overline{q}$ pair. In this case, the strict ordering in rapidity of baryon–antibaryon pairs, predicted by the model described in the previous item, is broken by a meson M ("popcorn" model, fig. 1d).

Contributions from the decays of heavier baryons, or of B mesons, must be added to the above processes.

The measurement of inclusive cross sections for baryon production does not display a high discriminating power among different models, since in general the simulation programs that incorporate such models contain adjustable parameters that can account for the observations.

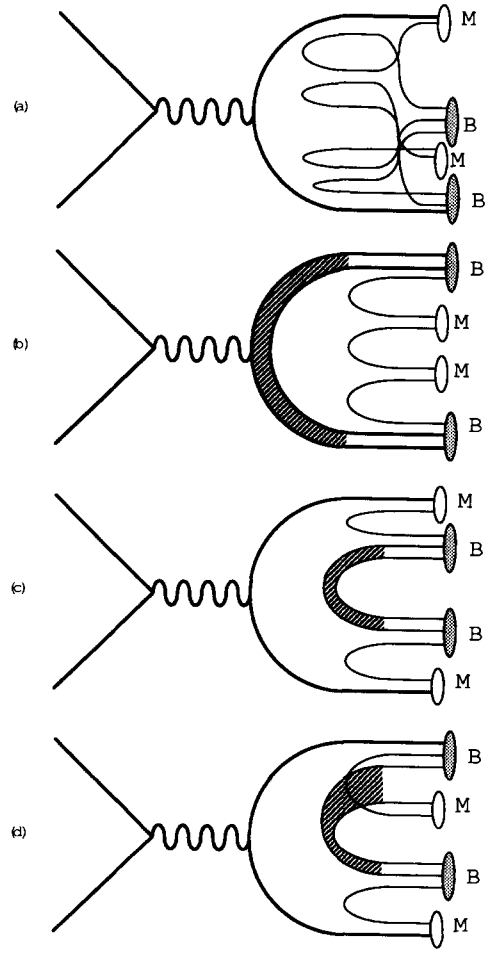

Fig. 1. Different models for baryon production: (a) recombination of quarks, (b) leading diquarks, (c) diquarks in fragmentation, (d) diquarks in fragmentation with "popcorn" contribution.

It is thus important to look at baryon correlations to distinguish among different models. The existence of short-range baryon–antibaryon correlations has been demonstrated experimentally at PEP/PETRA energies [1,2]. This means that $p\bar{p}$ pairs are more likely to occur close in phase space than far apart. Leading diquarks (or leading baryon pairs) are thus not a major source of baryon production (at least at PEP/PETRA energy, and presumably at higher energies too). The recombination model (i) is disfavoured by TASSO results [3].

In this paper, the production of the strange baryon Λ [#1] and the correlations between Λ and $\bar{\Lambda}$ produced in the same event have been analysed using data collected by the DELPHI detector [4] at the e^+e^- storage ring LEP at CERN. The data were taken at the Z^0 peak in 1991 and 1992. The cross section and the correlation measurements are compared with the predictions of the JETSET 7.3 Monte Carlo implementation of the Lund model (using parton shower generation and string fragmentation) with parameters related to baryon production tuned to data at PEP/PETRA energies [5], and with the HERWIG Monte Carlo implementation of the Webber-Marchesini model, version 5.4 [6].

The inclusive differential cross section for the production of the Λ baryon at the Z^0 peak has been studied previously by DELPHI [7] and OPAL [8] at LEP. OPAL [9] has recently published results on strange baryon correlations.

The present work extends the results of ref. [7], using ten times as many reconstructed Λ. The results on $\Lambda\bar{\Lambda}$ correlations are based on a number of pairs roughly ten times larger than those available at PEP/PETRA energies [10].

2. Experimental procedure and event selection

A description of the apparatus can be found in ref. [4]. Features of the apparatus relevant for the analysis of multi-hadronic final states (with emphasis on the detection of charged particles) are outlined in ref. [11]. The analysis presented here relied on the information provided by the central tracking detectors: the Micro Vertex Detector (VD), the Inner Detector (ID), the Time Projection Chamber (TPC), the Outer Detector (OD) and the Barrel Ring Imaging Cherenkov Detector (RICH).

- The VD consisted in 1991 and 1992 of 3 cylindrical layers of silicon, at radii 6.3, 9.0 and 11.0 cm. They measure $R\phi$ (i.e., transverse to the beam) coordinates over a length along the beam of 24 cm. The polar angle coverage of the VD is from 42° to 138°.

- The ID is a cylindrical drift chamber (inner radius 12 cm and outer radius 22 cm) covering polar angles between 29° and 151°.

- The TPC, the principal tracking device of DELPHI, is a cylinder of 30 cm inner radius, 122 cm outer radius and has a length of 2.7 m. Each end-cap is divided into 6 sector plates, each with 192 sense wires used for the particle identification. The energy loss per unit length of a charged particle (dE/dx) is measured by these wires as the 80% truncated mean of the amplitudes of the wire signals. A dE/dx measurement is considered to be significant if at least 30 wires contribute to it. About 25% of the tracks with momentum, p, above 1 GeV/c have no dE/dx information because they are too close to another track to separate them, or because they have too few wire hits.

- The OD consists of 5 layers of drift cells at radii between 192 and 208 cm, covering polar angles between 43° and 137°.

- The Barrel RICH [4] covers the polar angle between 40° and 140°. It identifies the charged particles by measuring the angle of emission of Cherenkov light, and thus the velocity. The mass of the charged particle is then extracted by using the velocity information combined with the momentum measurement. In order to cover a large momentum range (1 to 20 GeV/c), the DELPHI Barrel RICH uses two different Cherenkov radiators; one liquid (C_6F_{14}) and one gaseous (C_5F_{12}).

The central tracking system of DELPHI covers the region between 25° and 155° in polar angle, θ. The average momentum resolution for the charged particles in hadronic final states is in the range $\Delta p/p \simeq 0.001p$ to $0.01p$ (p in GeV/c), depending on which detectors are included in the track fit.

Charged particles were used in the analysis if they had:

(a) momentum larger than 0.1 GeV/c;

[#1] Unless otherwise stated, antiparticles are implicitly included.

(b) measured track length in the TPC greater than 25 cm;

(c) θ between 25° and 155°;

(d) relative error on the measured momentum smaller than 100%.

Hadronic events were then selected by requiring that:

(α) the total energy of the charged particles in each hemisphere (θ above and below 90°) exceeded 3 GeV;

(β) the total energy of the charged particles exceeded 15 GeV;

(γ) there were at least 5 charged particles with momenta above 0.2 GeV/c.

In the calculation of the energies, all charged particles have been assumed to have the pion mass.

A total of 993 287 events satisfied these cuts. Events due to beam-gas scattering and to $\gamma\gamma$ interactions have been estimated to be less than 0.1% of the sample; background from $\tau^+\tau^-$ events was calculated to be less than 0.2%.

The influence of the detector on the analysis was studied with the simulation program DELSIM [12]. Events were generated with the JETSET 7.3 Parton Shower Monte Carlo program [5] (JETSET PS in the following) with parameters tuned as in ref. [13]. The particles were followed through the detailed geometry of DELPHI giving simulated digitizations in each detector. These data were processed with the same reconstruction and analysis programs as the real data. Simulations based on HERWIG 5.4 (HERWIG in the following), based on the decays of clusters, were also used.

3. Λ production

The Λ baryons are detected by their decay in flight into $p\pi^-$. Such decays are separated from the primary Z^0 decay (primary vertex).

Candidate secondary decays, V_Λ, were found by considering all tracks pairs with opposite charge. The vertex defined by each such pair was determined such that the χ^2 obtained from the distances of the vertex to the extrapolated tracks was minimized.

The Λ decay vertex candidates were required to satisfy the following:

- In the $R\phi$ plane, the angle between the vector sum of the charged particle momenta and the line joining the primary to the secondary vertex was less than $(10 + 20/p_t(\Lambda))$ mrad, where $p_t(\Lambda)$ is the transverse momentum of the Λ candidate relative to the beam axis, in GeV/c.

- The radial separation of the primary and secondary vertex in the $R\phi$ plane was greater than 1 cm.

- When the reconstructed decay point of the Λ was beyond the VD radius, there were no signals in the VD consistent with association to the decay tracks.

- The probability of the χ^2 fit to the secondary vertex was larger than 0.02.

- The track impact parameter (with respect to the primary vertex) of the higher momentum particle was larger than 150 μm/$p_t(\Lambda)$.

- When dE/dx information was available, the dE/dx of the candidate proton p was within three standard deviations of the expected value.

Ambiguities occur with K^0 decays into $\pi^+\pi^-$ and with conversions of photons to e^+e^- pairs. The K^0_S background was reduced by rejecting $p\pi$ candidates whose mass, when taken as $\pi\pi$, was less than 3 standard deviations from the K^0_S mass. Photon conversions to e^+e^- pairs were mostly excluded by requiring the pair mass to be greater than 0.1 GeV/c^2 (assigning the electron mass to each particle) and by requiring the decay particles to have transverse momentum larger than 0.04 GeV/c with respect to the vector sum of their momenta.

The cuts listed above are designed to remove Λ's from secondary interactions in the detector, as well as combinatorial or physical (misidentified K^0's and photons) background. They discriminate also against Λ's coming from the decays of long-lived strange baryons, such as Ξ and Ω.

The $p\pi^-$ invariant mass spectrum from the accepted V_Λ candidates is shown in fig. 2; a clear Λ signal is seen, with a resolution of about 2.4 MeV/c^2. The average reconstruction efficiency for the detection of a decay $\Lambda \to p\pi$ was estimated by simulation to be about 18%.

The spectrum has been fitted using the MINUIT [14] package to the sum of two Gaussian functions for the signal, superimposed on a linear background in the range from 1.1 to 1.18 GeV/c^2. The fit gives $m_\Lambda = 1115.1 \pm 0.02$ (stat) ± 0.2 (syst) MeV/c^2 (consistent with the world average of 1115.63 ± 0.05 MeV/c^2 [15]), with a total of $42\,785 \pm 234$ (stat) $\pm$ 1500 (syst) Λ's. The systematic errors include con-

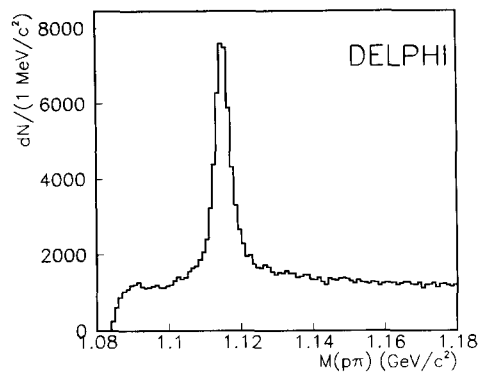

Fig. 2. pπ invariant mass spectrum for secondary decay candidates.

tributions from replacing the linear background parametrization by a third-order polynomial or an exponential with threshold, by using a Breit–Wigner shape to represent the signal, and from changing the mass range used for the fit.

The Λ lifetime, τ_Λ, has been determined from the selected sample. The correction factors for each bin of proper time are calculated from the simulation. A least-square fit of the corrected experimental distribution to an exponential decay function gives $\tau_\Lambda = 267 \pm 1$ ps (the error is statistical only), compared with the world average of 263 ± 2 ps [15]. Another consistency check was to measure if there were differences in the number of Λ and $\overline{\Lambda}$. The measured ratio $N_\Lambda/N_{\overline{\Lambda}}$ is 1.06 ± 0.02, consistent with the value of 1.05 ± 0.02 found in the simulation. It is expected that secondary interactions lead to a $\Lambda/\overline{\Lambda}$ ratio greater than 1.

The momentum-dependent efficiency for Λ reconstruction, including detector acceptance effects, has been calculated by the detailed simulation. The combinatorial background was subtracted for each region of momentum fraction x_p independently; the widths of the Gaussians were allowed to vary independently for each interval of x_p. The measured differential cross section $(1/\sigma_h)\mathrm{d}\sigma/\mathrm{d}x_p$ (where σ_h is the total hadronic cross section) for inclusive Λ and $\overline{\Lambda}$ production at the Z^0 is shown in table 1. The errors on the differential cross section include both the statistical and the systematic contributions; the systematic error comes mainly from the parametrization of the background in each x_p region. The results are consistent with our previous measurement [7].

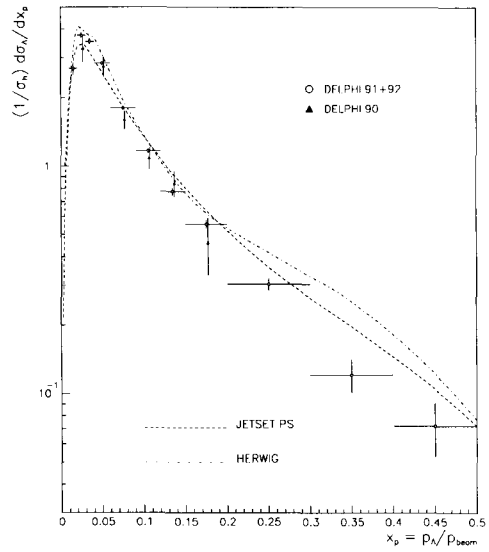

Fig. 3. Differential cross section for Λ production (open circles) as a function of the momentum fraction x_p, compared to the predictions of JETSET PS (dashed line), HERWIG (dashed-dotted line), and with the results previously published by DELPHI (closed triangles).

Table 1
Differential cross section for Λ production, as a function of the fractional momentum x_p.

$x_p = 2p/\sqrt{s}$	$(1/\sigma_h)\mathrm{d}\sigma/\mathrm{d}x_p$
0.01–0.02	2.69±0.16
0.02–0.03	3.76±0.09
0.03–0.04	3.54±0.10
0.04–0.06	2.84±0.05
0.06–0.09	1.80±0.04
0.09–0.12	1.17±0.03
0.12–0.15	0.774±0.032
0.15–0.20	0.555±0.025
0.20–0.30	0.303±0.019
0.30–0.40	0.121±0.020
0.40–0.50	0.072±0.019

In fig. 3 the measured cross section is compared with the prediction from JETSET PS and HERWIG. Both models, when taken with their default parameters, fail to reproduce quantitatively the spectrum at high momentum.

The mean Λ multiplicity, $\langle N_\Lambda \rangle + \langle N_{\overline{\Lambda}} \rangle$, was obtained by integrating the distribution as a function of x_p, cor-

recting for the unseen decay mode ($n\pi^0$), and assuming the unmeasured regions of x_p contain the same fraction of Λ as predicted by JETSET PS. This gave

$$\langle N_\Lambda \rangle + \langle N_{\bar{\Lambda}} \rangle = 0.357 \pm 0.003\ (\text{stat}) \pm 0.017\ (\text{syst}). \quad (1)$$

The systematic error reflects the uncertainties due to:

- The choice of the background parametrization. This generates an error of ± 0.004.
- The JETSET PS extrapolation. The average number of Λ in the unobserved region is about 0.012 according to the simulation; the relative uncertainty on this number was set to 100%.
- The Λ's produced by the decay of other particles. According to JETSET PS, approximately 40% of the Λ's come directly from fragmentation, 15% from the decay of the Σ^0, 28% from the decay of the $\Sigma^{*\pm}$ or of the Σ^{*0}, 14% from the decay of the Ξ^- or of the Ξ^0, and 4% from the decay of the Λ_c. The $\Sigma^{*\pm}(1385)$ rate might be overestimated by a factor of 2 in JETSET [8]. Inaccurate modelling in the simulation of the production ratios of secondary Λ's may affect the efficiency calculations. An uncertainty of 5% of the expected number of non-direct Λ's was assigned to this source, giving to the systematic error a contribution of ± 0.011.

The result agrees with the previous determination by DELPHI [7] ($0.36 \pm 0.03 \pm 0.06$) and with the determination by OPAL [8] ($0.351 \pm 0.003 \pm 0.019$). JETSET PS with default parameters predicts a value of 0.373, while HERWIG predicts 0.416.

4. $\Lambda\bar{\Lambda}$ correlations

The correlations between Λ and $\bar{\Lambda}$ produced in the same event were studied by searching for events with $\Lambda\bar{\Lambda}$ pairs ("unlike type"), and $\Lambda\Lambda$ or $\bar{\Lambda}\bar{\Lambda}$ pairs ("like type").

Two different methods of analysis were used for this purpose, which are described in detail in subsections 4.1 and 4.2.

The selection criteria for Λ's are different from those used to obtain the Λ inclusive differential cross sections. They were tuned in order to obtain the maximum efficiency within each method.

Furthermore, in order to ensure containment of the event in the fiducial volume of the detector, only hadronic events with the thrust axis in the barrel region were retained. It was required that $|\cos\theta_{\text{thrust}}| < 0.8$, where θ_{thrust} is the thrust axis polar angle. This reduces the number of hadronic events to approximately 85% of the total.

In both methods applied for studying the correlations, care was taken not to use pairs of V_0's which share a common track.

4.1. Method 1

The motivation for the selection criteria was to achieve a flat or linear background in the region of the Λ mass peak. The Λ decay candidates were required to satisfy the following:

(i) The χ^2 probability of the secondary vertex fit was greater than 1%.

(ii) The decay distance, normalized to the measurement error, was larger that 4σ, if the V_0 tracks had hits in the vertex detector (VD) and 6σ if the V_0 is outside the VD.

(iii) When the information of the dE/dx was available from the TPC, the highest momentum track (defined as the proton) had a dE/dx within 3σ of the proton hypothesis, and the other track was consistent with a pion within 3σ from the expected value.

(iv) The difference between the flight direction and the vector sum of the two tracks of the V_0 was less than the minimum of the two values: 30 mrad and $(10 + 20/p_t)$ mrad, where the p_t of the V_0 (in the $R\phi$ plane) was expressed in GeV/c.

(v) The probability: $1 - \exp(-(m_\Lambda/p_t)(r_{R\phi}/c\tau_\Lambda))$ that the Λ had decayed within the radius $r_{R\phi}$ was larger than 4% and smaller than 98%.

(vi) The opening angle between the two tracks in the $R\phi$ plane was less than 0.6 rads.

(vii) The momentum of the V_0 was larger than 0.5 MeV/c.

(viii) The p_T of the decay products relative to the V_0 direction was larger than 0.02 GeV/c.

(ix) The mass of the V_0, assuming that both tracks are π's, was more than three standard deviations from the K^0 mass.

The efficiency was studied using the detailed DELPHI simulation programs (see section 2) and was found to be 17% for 1991 data and 18% for the 1992.

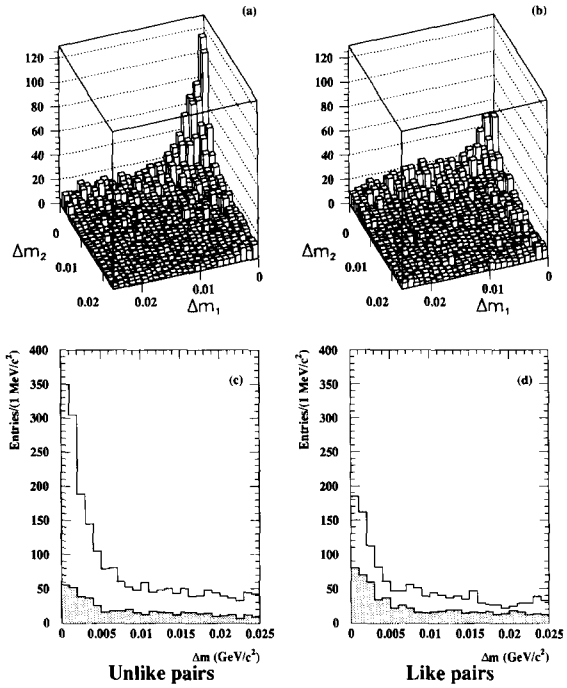

Fig. 4. Scatter plot of the differences in $p\pi$ invariant mass with respect to the nominal Λ mass for (a) unlike type pairs and (b) like type pairs. Projection of the slice $\Delta m_2 < 5$ MeV/c^2 on the the Δm_1 axis for (c) unlike type pairs and (d) like type pairs. The shaded area indicates the projection onto the Δm_1 axis of the slice 10 MeV/c^2 $< \Delta m_2 <$ 25 MeV/c^2, scaled down by the factor $k = 3$, as explained in the text.

It varies from approximately 2%(1%) at around 0.5 GeV/c to 30%(27%) at around 3 GeV/c and drops to about 10%(9%) at 15 GeV/c for 1992 and 1991 data respectively.

First, events have been searched for with at least two candidate Λ, separating unlike type pairs from like type pairs.

To evaluate the backgrounds in these samples, the absolute values Δm_1 and Δm_2 of the differences between the two V_Λ candidates' invariant masses $m(p\pi)$ and the known Λ mass value of 1.1156 GeV/c^2 were computed. The correlations between Δm_1 and Δm_2 are shown in figs. 4a and 4b for unlike and like type pairs respectively. The peaks at low values of Δm_1 and Δm_2 in both plots are an indication of the production of both unlike and like type pairs.

The "signal region", defined by $\Delta m_1, \Delta m_2 < a =$ 5 MeV/c^2, contains 1 004 events with unlike type candidate pairs and 527 events with like type candidate pairs. The number N of selected pairs is a sum of four contributions:

- N_{tt}, the number of pairs of true $\Lambda(\bar{\Lambda})$;
- N_{tf}, the number of pairs in which the first candidate is a true $\Lambda(\bar{\Lambda})$, while the second is fake;
- N_{ft}, the number of pairs in which the first candidate is a fake $\Lambda(\bar{\Lambda})$, while the second is true;
- N_{ff}, the number of pairs in which neither candidate is a true $\Lambda(\bar{\Lambda})$.

It was verified by simulation that, in the region of Δm used for the extrapolation, the background under the Δm_i peak is flat for each $\Lambda(\bar{\Lambda})$ candidate. The three background contributions N_{tf}, N_{ft} and N_{ff} can thus be estimated from the numbers of pairs N_1, N_2 and N_3, in three "control regions" defined in the Δm_1, Δm_2 correlation plots:

$$N_1 = kN_{\mathrm{ft}} + kN_{\mathrm{ff}},$$

$$\Delta m_2 < a, \quad b < \Delta m_1 < b + ka$$

$$N_2 = kN_{\mathrm{tf}} + kN_{\mathrm{ff}},$$

$$\Delta m_1 < a, \quad b < \Delta m_2 < b + ka,$$

$$N_3 = k^2 N_{\mathrm{ff}},$$

$$b < \Delta m_1 < b + ka, \quad b < \Delta m_2 < b + ka.$$

The upper limit $a = 5\,\mathrm{MeV}/c^2$ of the signal region, the lower limit $b = 10\,\mathrm{MeV}/c^2$ and the width $ka = 15\,\mathrm{MeV}/c^2$ of the interval defining the control region were chosen to have a stable signal to background ratio and to match the hypothesis of a flat background behaviour for the extrapolation procedure.

These choices are illustrated in figs. 4c and 4d, for unlike and like type pairs respectively. The histogram is obtained projecting the slice $\Delta m_2 < a$ onto the Δm_1 axis. For $\Delta m_1 < a$, it therefore shows the total number N of events in the signal region. For $b < \Delta m_1 < b + ka$, it also shows the contents of the first control region $N_1 = kN_{\mathrm{ft}} + kN_{\mathrm{ff}}$. The shaded area indicates the projection onto the Δm_1 axis of the slice $b < \Delta m_2 < b + ka$, scaled down by the factor k. It thus shows the background contribution $N_2/k = N_{\mathrm{tf}} + N_{\mathrm{ff}}$, scaled from the second control region, to the events in the signal region ($\Delta m_1 < a$). It also shows the

contribution $N_3/k = kN_{ff}$ of fake-fake pairs, scaled from the third control region, for $b < \Delta m_\Lambda < b + ka$.

The number of true pairs in the signal region can then be estimated as

$$N_{tt} = N - (N_{tf} + N_{ft} + N_{ff})$$
$$= N - (N_1 + N_2)/k + N_3/k^2,$$

giving finally after background subtraction $661 \pm 36(\text{stat}) \pm 25(\text{syst})$ $\Lambda\overline{\Lambda}$ pairs and $188 \pm 26(\text{stat}) \pm 13(\text{syst})$ $\Lambda\Lambda$ or $\overline{\Lambda\Lambda}$ pairs.

After corrections for acceptance and reconstruction efficiencies, the average multiplicities per hadronic event were obtained:

$$\langle N_{\Lambda\Lambda}\rangle + \langle N_{\overline{\Lambda\Lambda}}\rangle$$
$$= 0.018 \pm 0.004(\text{stat}) \pm 0.004(\text{syst}), \quad (2)$$

$$\langle N_{\Lambda\overline{\Lambda}}\rangle = 0.090 \pm 0.005(\text{stat}) \pm 0.007(\text{syst}). \quad (3)$$

The systematics were evaluated by a variation of the signal region upper limit from $a = 5$ MeV/c^2 to $a = 6$ MeV/c^2, and of the control region from the range between 10 and 15 MeV/c^2 off the mass peak, to the range between 20 and 25 MeV/c^2 off the mass peak. The systematic error from the extrapolation to the unseen momentum region was added in quadrature.

These results are consistent with the corresponding measurements from OPAL [9], $\langle N_{\Lambda\overline{\Lambda}}\rangle - (\langle N_{\Lambda\Lambda}\rangle + \langle N_{\overline{\Lambda\Lambda}}\rangle) = 0.0621 \pm 0.0034 \pm 0.0084$, and $\langle N_{\Lambda\Lambda}\rangle + \langle N_{\overline{\Lambda\Lambda}}\rangle = 0.0205 \pm 0.0039 \pm 0.0028$.

In figs. 5a1 and 5b1 the corrected distributions of rapidity difference and angular separation in the laboratory frame are presented for the $\Lambda\overline{\Lambda}$ pairs. Rapidities were computed with respect to the sphericity axis of the hadronic events. In these distributions, the background has been subtracted bin by bin as explained above. The differential cross sections for unlike pairs, as a function of the difference in rapidity and of the cosine of the angle α of the pair (measured in the laboratory), are shown in table 2 and table 3 respectively. To account for systematic errors coming from the background subtraction, the error of the differential cross section in each bin has been obtained by summing the statistical and systematic uncertainties in quadrature.

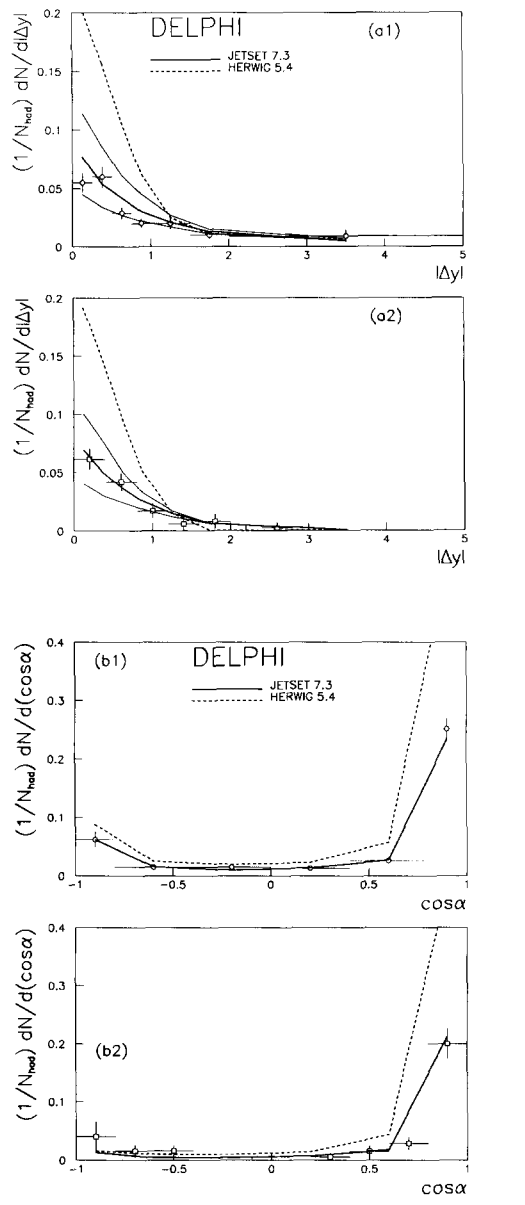

Fig. 5. (a1) Differential cross section for the production of $\Lambda\overline{\Lambda}$ pairs (Method 1), as a function of the difference Δy in rapidity, compared to the predictions of JETSET PS (solid lines) with popcorn probability = 50% (bold), no popcorn (upper), popcorn probability = 90% (lower), and HERWIG (dashed line). (a2) Same as (a1), for correlated $\Lambda\overline{\Lambda}$ pairs (Method 2). JETSET PS default (50% popcorn). (b1) Same as (a1), as a function of the cosine of the angle α between the Λ and the $\overline{\Lambda}$ (Method 1). (b2) Same as (b1), for correlated $\Lambda\overline{\Lambda}$ pairs (Method 2). JETSET PS default (50% popcorn).

Table 2
Differential cross section for $\Lambda\overline{\Lambda}$ production, as a function of the difference in rapidity Δy. Systematic errors are included in the uncertainties.

Δy	$(1/\sigma_h)\mathrm{d}\sigma_{\Lambda\overline{\Lambda}}/\mathrm{d}(\Delta y)$
0.00–0.25	0.055 ± 0.008
0.25–0.50	0.060 ± 0.009
0.50–0.75	0.029 ± 0.005
0.75–1.00	0.020 ± 0.004
1.00–1.50	0.020 ± 0.005
1.50–2.00	0.010 ± 0.003
2.00–5.00	0.009 ± 0.005

Table 3
Differential cross section for $\Lambda\overline{\Lambda}$ production, as a function of the cosine of the angle α between the the Λ and the $\overline{\Lambda}$ in the laboratory frame. Systematic errors are included in the uncertainties.

$\cos\alpha$	$(1/\sigma_h)\,\mathrm{d}\sigma_{\Lambda\overline{\Lambda}}/\,\mathrm{d}(\cos\alpha)$
−1.0– −0.8	0.062 ± 0.013
−0.8– −0.4	0.015 ± 0.005
−0.4– 0.0	0.015 ± 0.005
0.0– 0.4	0.013 ± 0.003
0.4– 0.8	0.026 ± 0.005
0.8– 1.0	0.251 ± 0.018

Figs. 5a and 5b display a strong $\Lambda\overline{\Lambda}$ correlation close in phase space. This is inconsistent with the recombination model, which predicts no dynamical correlations, and with the dominance of leading diquarks, which would produce a distribution peaked at $\cos\alpha = -1$.

In JETSET PS the "popcorn" mechanism [16] attenuates the baryon–antibaryon correlation by the insertion of mesons, according to a parameter ρ_{popcorn}, such that the probability of having a meson between a baryon B and an antibaryon $\overline{\mathrm{B}}$, $P(\mathrm{BM}\overline{\mathrm{B}})/[P(\mathrm{B}\overline{\mathrm{B}}) + P(\mathrm{BM}\overline{\mathrm{B}})]$, is roughly equal to $\rho/(0.5+\rho)$. Our data indicate that popcorn improves the agreement in the description of the $\Lambda\overline{\Lambda}$ correlations within JETSET.

Both the average number of $\Lambda\overline{\Lambda}$ pairs per hadronic event and the rapidity difference distribution can be compared with the predictions of JETSET PS. The normalized ratio of unlike pairs to single Λ, $\lambda = 2\langle N_{\Lambda\overline{\Lambda}}\rangle/(\langle N_\Lambda\rangle + \langle N_{\overline{\Lambda}}\rangle)$, is measured as

$$\lambda = 0.50 \pm 0.03(\mathrm{stat}) \pm 0.05(\mathrm{syst}), \qquad (4)$$

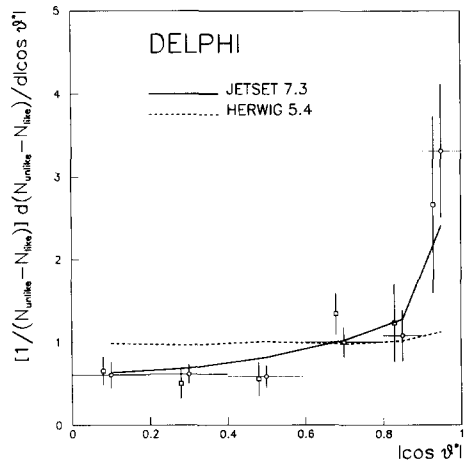

Fig. 6. Distribution of $\Lambda\overline{\Lambda}$ pairs in the cosine of the angle ϑ^* between the Λ direction and the sphericity axis, after subtraction of like-sign combinations. Open circles (Method 1) and open squares (Method 2). Predictions from JETSET PS (solid line) and HERWIG (dashed line). Distributions normalized to 1.

consistent with the value of 0.48 ± 0.10 measured at PEP/PETRA [17], and with the value of 0.46 predicted by JETSET PS default. HERWIG with default parameters predicts $\lambda = 0.82$, which is higher than the DELPHI measurement.

Baryon–antibaryon correlations can be used for distinguishing between string fragmentation and cluster fragmentation models. These predict substantially different distributions of the angle ϑ^* between the momentum difference of a baryon–antibaryon pair, in its centre-of-mass system, and the sphericity axis. If the baryons are produced in the decays of unpolarized clusters with baryon number equal to 0, the distribution in $|\cos\vartheta^*|$ will be flat. In a string model, the momentum difference will tend to align with the sphericity axis, since baryon and antibaryon are pulled apart by the string tension.

Experimentally, there is a background from the combination of baryon pairs coming from different clusters, or different $\mathrm{D}\overline{\mathrm{D}}$ pairs. This contamination can be removed by subtracting like pairs, which should have this origin in both models.

The DELPHI results on the distribution of the unlike pairs in $|\cos\vartheta^*|$ is displayed in fig. 6, and compared with the predictions of a simulation based on cluster decay (HERWIG) and one based on string

fragmentation (JETSET). In order to account for the differences between model and data concerning the pair production rate, all distributions are normalized to unity.

The shape measured by DELPHI is clearly consistent with the predictions from string models, and excludes the hypothesis that the decay of unpolarized clusters with baryon number zero is the only source of $\Lambda\overline{\Lambda}$ pairs.

The measured distribution of $|\cos\vartheta^*|$ for like pairs was larger than zero by more than 1.5 standard deviations only in the region $|\cos\vartheta^*| > 0.9$. The yield of like pairs is thus consistent with the hypothesis that these come from different clusters (or different diquark–antidiquark systems). We have no indication of clusters splitting into dibaryon–antidibaryon systems, i.e., of like baryon pairs coming from the same cluster.

4.2. Method 2

This method is similar to the one used in ref. [9], and it differs from Method 1 in the way in which both the signal and the background are estimated.

The like sign pairs are taken as estimators of the uncorrelated pairs plus combinatorial background, and subtracted from the unlike sign pairs at the level of uncorrected distributions. It is important in this case that the combinatorial background in both the like and unlike pairs is the same and is kept as low as possible.

To this purpose, the following cuts were changed with respect to Method 1:

(viii) The p_T of the V_0 computed on the plane perpendicular to the V_0 direction was required to be larger than 0.04 and smaller than 0.2 GeV/c.

(ix) The mass of the V_0, assuming that both tracks were π's, was required to be at least 10 MeV/c^2 from the K^0 mass.

The following cuts were added:

(x) The ratio of the momentum of the higher momentum particle to that of the lower momentum particle was required to be greater than 3. This cut reduces the K^0 background and at the same time makes unambiguous the definition of a Λ or $\overline{\Lambda}$ (using the charge of the higher momentum track).

(xi) Whenever the Barrel RICH information was available, it was required that the higher momentum track (considered to be a proton) was not identified as a pion by the Barrel RICH. This cut was found to reject less than 0.05% of the signal, and at the same time to improve the signal to background ratio from 0.95 to 1.5 in the mass region 1106–1126 MeV/c^2. In the 1991 data the RICH selection was not included and instead the cut on the K^0 hypothesis was set to ± 15 MeV/c^2. The signal to background ratio for the 1991 data was 1.2.

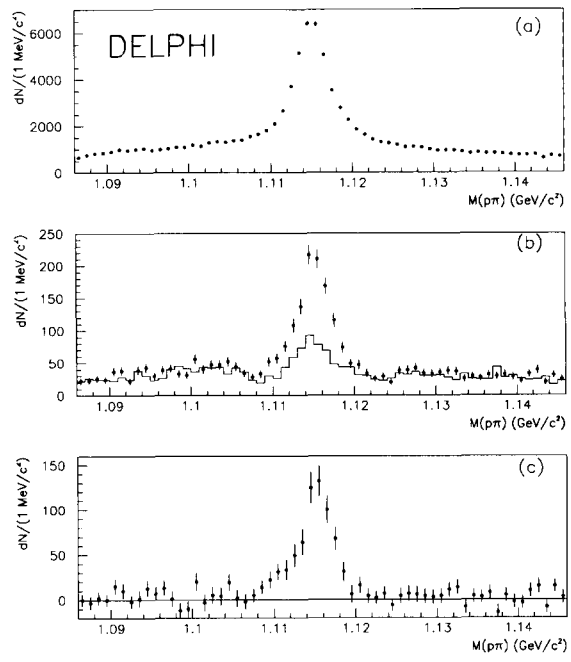

Fig. 7. (a) $p\pi$ invariant mass spectrum of the candidate Λ's in Method 2 (see text). (b) $p\pi$ invariant mass spectrum of events tagged by another Λ candidate, for like (solid line) and unlike (dots) combinations. (c) Difference unlike-like.

The inclusive $p\pi$ mass spectrum after these cuts is shown in fig. 7a. In the signal region (1106–1126 MeV/c^2), 33878 ± 241 (stat) Λ candidates were found after background subtraction.

For the $\Lambda\overline{\Lambda}$ correlations a Λ candidate was defined as a "tagger" when it was within ± 10 MeV/c^2 around the Λ mass for V_0's with x_p less than 0.2 and ± 15 MeV/c^2 for x_p larger than 0.2. When a "tagger" was found in an event, a second Λ candidate was searched for. In fig. 7b the mass spectrum of the second Λ is shown in the case of "unlike" pairs (points with the error bars) and in the case of "like" pairs (histogram). The agreement of the background for the two spectra is

excellent. The excess in the $\Lambda\bar{\Lambda}$ signal is an indication of correlated Λ's produced in the events. The signal of correlated "unlike" Λ pairs can be determined by the difference of the two spectra which is shown in fig. 7c. In the mass region (1106–1126 MeV/c^2), we find 752 ± 48 $\Lambda\bar{\Lambda}$ pairs.

The number of $\Lambda\Lambda$ ($\bar{\Lambda}\bar{\Lambda}$) was computed from the spectrum of the second Λ in the like pairs (fig. 7b) as follows. The background under the mass peak was computed from the side bands. After subtraction the remaining signal still had to be corrected for events where the "tagger" Λ comes from the combinatorial background. This probability was taken from the inclusive Λ spectrum and was 40% and 45.5% for the 1992 and 1991 data respectively. After the background subtraction we have 188 ± 55 like pairs.

After correcting for acceptance efficiency and branching ratio to $p\pi$, and taking the weighted mean between the 1991 and 1992 values, we find the following average multiplicities per hadronic event:

$$\langle N_{\Lambda\Lambda}\rangle + \langle N_{\bar{\Lambda}\bar{\Lambda}}\rangle = 0.017 \pm 0.004(\text{stat}) \pm 0.003(\text{syst}), \quad (5)$$

$$\langle N_{\Lambda\bar{\Lambda}}\rangle - (\langle N_{\Lambda\Lambda}\rangle + \langle N_{\bar{\Lambda}\bar{\Lambda}}\rangle) = 0.068 \pm 0.004(\text{stat}) \pm 0.008(\text{syst}). \quad (6)$$

The main sources of systematic error considered were the systematic uncertainty in efficiency and in the background subtraction. From these sources, a relative systematic uncertainty of about 11% for the mean number of $\Lambda\bar{\Lambda}$ pairs and 17% for the $\Lambda\Lambda$ ($\bar{\Lambda}\bar{\Lambda}$) was estimated.

The normalized ratio of unlike correlated pairs to single Λ's, $\lambda' = 2(\langle N_{\Lambda\bar{\Lambda}}\rangle - (\langle N_{\Lambda\Lambda}\rangle + \langle N_{\bar{\Lambda}\bar{\Lambda}}\rangle))/(\langle N_{\Lambda}\rangle + \langle N_{\bar{\Lambda}}\rangle)$, is measured as

$$\lambda' = 0.38 \pm 0.02(\text{stat}) \pm 0.05(\text{syst}). \quad (7)$$

This corresponds, through eqs. (5) and (6), to

$$\lambda = 0.48 \pm 0.03(\text{stat}) \pm 0.05(\text{syst}). \quad (8)$$

In figs. 5a2, 5b2 and 6 (open squares), the background subtracted and efficiency corrected distributions of the unlike correlated $\Lambda\bar{\Lambda}$ pairs are given for Δy, $\cos\alpha$ and $|\cos\vartheta^*|$ respectively (see the previous subsection for the definitions). It was found that the detection efficiency for the Λ's depends only on their momentum. Thus the correction for efficiency was done according to the momentum of the Λ. It was also verified that the efficiency to detect a second Λ in the event was the same as that for a single Λ.

The conclusions to be drawn from the plots are the same as for Method 1. The results from the two methods are consistent.

5. Summary and Conclusions

The inclusive production of the Λ baryon and the correlations between Λ and $\bar{\Lambda}$ produced in the same event have been studied in a sample of about 993 000 hadronic Z^0 decays collected by the DELPHI detector at LEP.

The following average multiplicities have been measured [#2]:

$$\langle N_{\Lambda}\rangle + \langle N_{\bar{\Lambda}}\rangle = 0.357 \pm 0.017, \quad (9)$$

$$\langle N_{\Lambda\Lambda}\rangle + \langle N_{\bar{\Lambda}\bar{\Lambda}}\rangle = 0.018 \pm 0.006, \quad (10)$$

$$\langle N_{\Lambda\bar{\Lambda}}\rangle = 0.090 \pm 0.009, \quad (11)$$

$$\lambda = 2\frac{\langle N_{\Lambda\bar{\Lambda}}\rangle}{\langle N_{\Lambda}\rangle + \langle N_{\bar{\Lambda}}\rangle} = 0.50 \pm 0.06. \quad (12)$$

The predictions of the JETSET 7.3 version of the Lund Monte Carlo program, with default parameters, are consistent with these results, while HERWIG 5.4 with default parameters overestimates the production of Λ and the $\Lambda\bar{\Lambda}$ correlation. Both JETSET PS and HERWIG predict a production cross section at high momentum larger than observed.

The $\Lambda\bar{\Lambda}$ correlation is consistent with the prediction of models in which diquarks in fragmentation are the major baryon source. The "popcorn" mechanism is needed in JETSET with default parameters to correctly reproduce the observed correlations.

The distribution of ϑ^* (the angle between the momentum difference of unlike pairs in their centre-of-mass system and the sphericity axis) favours string models with respect to models based on the decay of unpolarized clusters with baryon number zero.

[#2] For the quantities quoted in these conclusions, statistical and systematic errors have been summed in quadrature.

Acknowledgement

We are greatly indebted to our technical collaborators and to the funding agencies for their support in building and operating the DELPHI detector, and to the members of the CERN-SL Division for the excellent performance of the LEP collider.

References

[1] TASSO Collab., M. Althoff et al., Phys. Lett. B 139 (1984) 126.
[2] TPC Collab., H. Aihara et al., Phys. Rev. Lett. 55 (1985) 1047.
[3] TASSO Collab, M. Althoff et al., Z. Phys. C 17 (1984) 5.
[4] DELPHI Collab., P. Aarnio et al., Nucl. Instrum. Methods A 303 (1991) 233.
[5] T. Sjöstrand, Comput. Phys. Commun. 27 (1982) 243; 28 (1983) 229; PYTHIA 5.6 and JETSET 7.3, CERN-TH.6488/92, September 1992.
[6] G. Marchesini and B.R. Webber, Nucl. Phys. B 238 (1984) 1.
[7] DELPHI Collab., P. Abreu et al., Phys. Lett. B 275 (1991) 231.
[8] OPAL Collab., G. Alexander et al., Phys. Lett. B 291 (1992) 503.
[9] OPAL Collab., P.D. Acton et al., Phys. Lett. B 305 (1993) 415.
[10] For reviews see for example: D.H. Saxon, Baryon production in e^+e^- Annihilations, RAL-88-102; A. De Angelis, Baryon production in e^+e^-Annihilations, CERN-PPE/93-35, to be published in J. Phys. G.
[11] DELPHI Collab., P. Aarnio et al., Phys. Lett. B 240 (1990) 271.
[12] DELSIM User's Guide, DELPHI 89-15 PROG 130, CERN, February 1989;
DELSIM Reference Manual, DELPHI 89-68 PROG 143, CERN, September 1989.
[13] W. de Boer et al., IEKP-KA/91-07, Karlsruhe, June 1991.
[14] F. James and M. Roos, CERN Program Library D506;
MINUIT - Function Minimization and Error Analysis.
[15] Particle Data Group, Review of Particle Properties, Phys. Rev. D 45, Part II (1992).
[16] B. Andersson, G. Gustavson and T. Sjöstrand, Phys. Scr. 32 (1985) 544.
[17] J. Ojang, Inclusive Production and Flavour Correlations of Strange Baryons in e^+e^- Annihilations at 29 GeV, PhD Thesis at UCLA (1991).